

Hybrid Organic–Inorganic Perovskites on the Move

Published as part of the Accounts of Chemical Research special issue “Lead Halide Perovskites for Solar Energy Conversion”.

David A. Egger,^{*,†} Andrew M. Rappe,^{*,‡} and Leeor Kronik^{*,†}

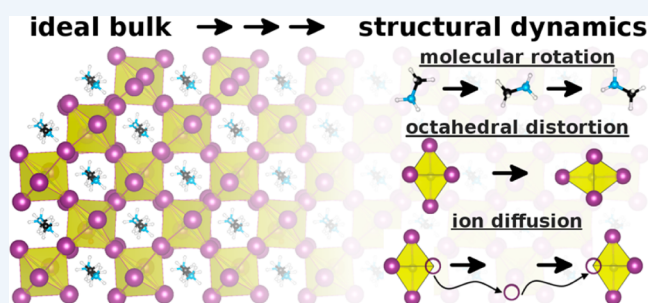
[†]Department of Materials and Interfaces, Weizmann Institute of Science, Rehovoth 76100, Israel

[‡]The Makineni Theoretical Laboratories, Department of Chemistry, University of Pennsylvania, Philadelphia, Pennsylvania 19104–6323, United States

CONSPECTUS: Hybrid organic–inorganic perovskites (HOIPs) are crystals with the structural formula ABX_3 , where A , B , and X are organic and inorganic ions, respectively. While known for several decades, HOIPs have only in recent years emerged as extremely promising semiconducting materials for solar energy applications. In particular, power-conversion efficiencies of HOIP-based solar cells have improved at a record speed and, after only little more than 6 years of photovoltaics research, surpassed the 20% threshold, which is an outstanding result for a solution-processable material. It is thus of fundamental importance to reveal physical and chemical phenomena that contribute to, or limit, these impressive photovoltaic efficiencies.

To understand charge-transport and light-absorption properties of semiconducting materials, one often invokes a lattice of ions displaced from their static positions only by harmonic vibrations. However, a preponderance of recent studies suggests that this picture is not sufficient for HOIPs, where a variety of structurally dynamic effects, beyond small harmonic vibrations, arises already at room temperature.

In this Account, we focus on these effects. First, we review structure and bonding in HOIPs and relate them to the promising charge-transport and absorption properties of these materials, in terms of favorable electronic properties. We point out that HOIPs are much “softer” mechanically, compared to other efficient solar-cell materials, and that this can result in large ionic displacements at room temperature. We therefore focus next on dynamic structural effects in HOIPs, going beyond a static band-structure picture. Specifically, we discuss pertinent experimental and theoretical findings as to phase-transition behavior and molecular/octahedral rearrangements. We then discuss atomic diffusion phenomena in HOIPs, with an emphasis on the migration of intrinsic and extrinsic ionic species. From this combined perspective, HOIPs appear as highly dynamic materials, in which structural fluctuations and long-range ionic motion have an unusually strong impact on charge-transport and optical properties. We highlight the potential implications of these effects for several intriguing phenomenological observations, ranging from scattering mechanisms and lifetimes of charge carriers to light-induced structural effects and ionic conduction.



1. INTRODUCTION

Hybrid organic–inorganic perovskites (HOIPs), the structure of which is defined below, are materials which are solution processable, comprise earth-abundant elements, and yet exhibit outstanding semiconducting and light-absorption properties (see refs 1–3 for overviews). These features render HOIPs promising for (opto-) electronic applications in general and photovoltaic (PV) devices in particular,^{4–7} as power-conversion efficiencies surpassed 20% after some 6 years of PV research.⁸ The microscopic origin of this success lies partly in the electronic structure of HOIPs, which is well understood:^{9,10} it resembles that of a good inorganic semiconductor, with optical gaps that can be close to optimal for solar absorption, small exciton binding energies, and low effective masses. This combination allows for efficient charge-carrier generation, transport, and collection.

In this Account, we first review the static structural and electronic properties of HOIPs. We then show that the static band-structure picture, possibly with harmonically vibrating ions, still leaves important phenomena, for example, light-induced effects or hysteresis in the current–voltage curves of HOIP solar cells, unexplained. We therefore focus on *dynamic structural effects* in HOIPs, highlighting important molecular and octahedral rearrangements, as well as ion migration phenomena, discuss how those could explain some of the remaining mysteries of HOIPs, and suggest further routes for progress.

Received: December 14, 2015

Published: February 15, 2016

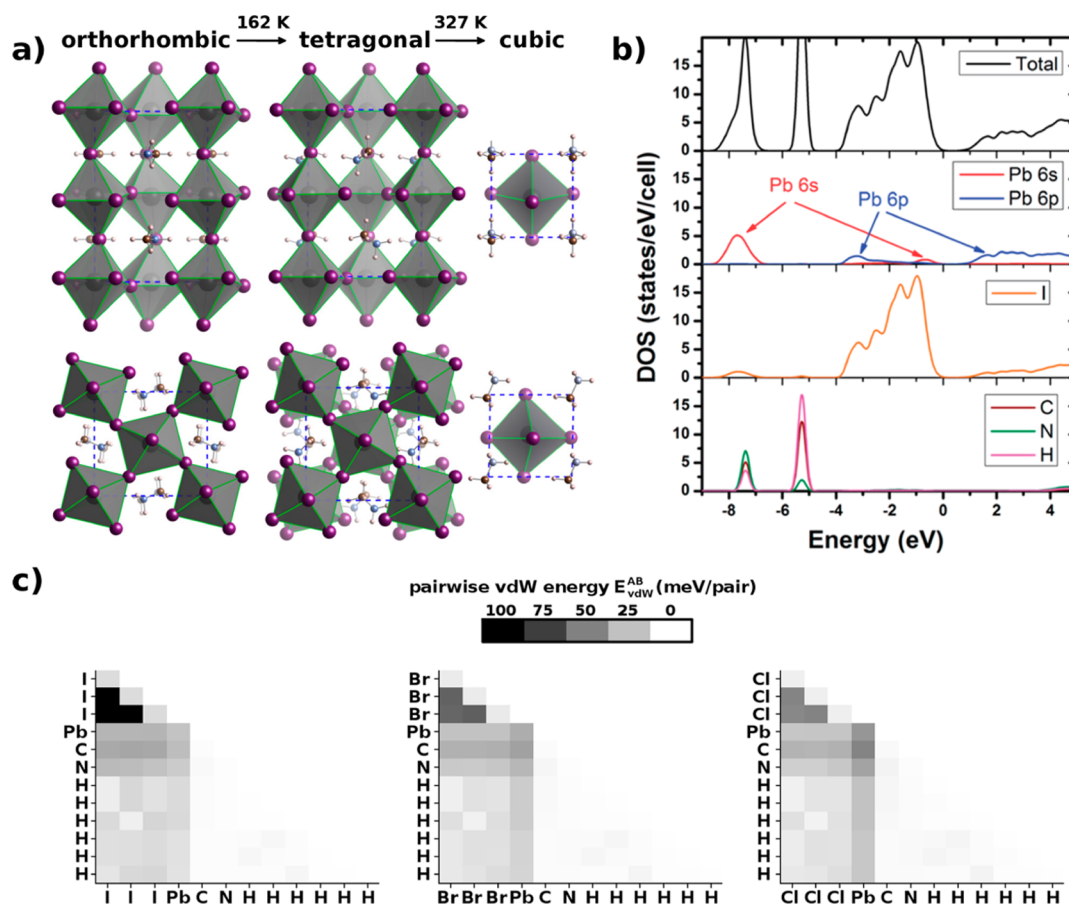


Figure 1. (a) Schematic representation of methylammonium lead iodide (MAPbI₃) and its crystal structures at different temperatures.¹⁶ Upper (lower) panels show side (top) views. Dashed lines represent unit cell boundaries. Phase-transition temperatures were taken from ref 18. Adapted with permission from ref 16. Copyright 2015 American Physical Society. (b) Total and projected density of states of tetragonal MAPbI₃, showing orbital-specific contributions.⁹⁰ Reproduced with permission from ref 90. Copyright 2014 The Royal Society of Chemistry. (c) Graphical summary of pairwise dispersive energies, $E_{\text{vdW}}^{\text{AB}}$, between atomic sites A and B in the unit cell of MAPbI₃ (left panel), MAPbBr₃ (center panel), and MAPbCl₃ (right panel).²⁶ Reproduced with permission from ref 26. Copyright 2014 American Chemical Society.

2. CRYSTAL STRUCTURE, BONDING, AND PHASE TRANSITIONS OF HOIPs

Perovskites possess the formula ABX_3 , where A, B, and X are ions that obey size restrictions quantified by the Goldschmidt tolerance factor:¹¹

$$t = \frac{r_A + r_X}{\sqrt{2}(r_B + r_X)}$$

where r_A , r_B , and r_X denote the ionic radii. When t is close to unity, the “aristotype” ideal cubic perovskite structure can form. It consists of corner-shared BX_6 octahedra and A-cations occupying the voids between them. When t significantly deviates from unity, perovskite motifs with edge- and face-sharing octahedra may be favored over the corner-sharing structure.¹²

Perovskites can adopt a wide variety of phases that typically involve small symmetry-breaking distortions of the aristotype,¹³ for example, octahedral tilts (characterized with Glazer’s notation¹⁴), A- and B-cation displacements, and their combinations. Many crystal structures and space groups are accessible from the aristotype, including polar space groups, that is, ferroelectric and antiferroelectric ones.¹⁵

In HOIPs, the A-site is occupied by a small organic cation (typically methylammonium, MA). Most HOIPs studied today have a divalent metallic atom (e.g., Pb or Sn) on the B-site and

halogens (I, Br, Cl) on the X-sites. Figure 1a shows a schematic of the prototypical MAPbI₃,¹⁶ described by Weber long ago,¹⁷ including the tetragonal and orthorhombic structures it adopts at lower temperatures (determined by X-ray diffraction, XRD).¹⁸ The molecular cation has a dipole moment and a symmetry lower than that of the (ideal) BX_6 octahedron. Neighboring molecules in HOIPs can, in principle, align in different ways over various length scales. Therefore, while t can still be ≈ 1 , one expects molecule-based symmetry breaking leading to a rich structural variety accessible at a given temperature. Indeed, density functional theory (DFT) calculations have shown that close to equilibrium many different structures are locally stable and differ in energy by only a few meV/formula unit.^{19–22} Phase diagrams and associated static and dynamic structural features of HOIPs can thus be particularly rich and interesting.

This diversity can be linked to cohesion in HOIPs, for which ionic bonding is a major driving force. This manifests itself in the electronic structure of HOIPs (e.g., MAPbI₃, see Figure 1b),^{23,90} characterized by an anionic (iodide) valence and cationic (lead) conduction band.^{9,10,23,90} The oxidation state of the X-ions in halide-based HOIPs is -1 (instead of -2 in oxide perovskites), and the Madelung potential is significantly less binding for HOIPs than for oxides.²⁴ Again using MAPbI₃ as an example, Pb and I also interact covalently to some extent,

especially due to interaction of lone-pair Pb 6s with I 5p electrons, contributing to the top of the valence band (Figure 1b).^{9,10,23,90} The species in HOIPs have large polarizabilities and can support significant dispersive interactions. Therefore, ordinarily weak interactions, notably van der Waals (vdW) interactions, and hydrogen bonding supported by the organic cation, also play an important role for the structure of HOIPs, especially given relatively weak electrostatic binding.^{25–27} Accordingly, first-principles calculations demonstrated the importance of vdW-interactions among the inorganic atoms^{25–27} and H-bonding between the organic moieties and inorganic octahedra (Figure 1c).²⁶

Significant contributions of the organic cation to the HOIP band structure are found only at several eV below the valence band maximum (Figure 1b),^{9,10,23,90} that is, beyond H-bonding there is essentially no hybridization between the organic and inorganic part of HOIPs. Instead, the molecule acts as a scaffold, big enough so that lead-halide perovskites can form (with favorable t) close to room temperature. The large size of MA is important, because the analogous all-inorganic, CsPbI₃, adopts the edge-sharing NH₄CdCl₃ structure at ambient conditions rather than the cubic perovskite one, with a significantly different electronic structure that is less favorable for photovoltaics.³

The above considerations suggest that chemical bonds are not stiff in HOIPs. Indeed, lattice constants of ideal cubic MAPbX₃ span 5.7–6.3 Å, significantly larger than the 3.8–4.2 Å common for oxide perovskites.¹³ Furthermore, experimental and theoretical Young and bulk moduli of different HOIPs^{26,28–31} are between ≈ 10 and 25 GPa, that is, at least tens of GPa smaller than values for typical oxide perovskites or inorganic semiconductors. This means that HOIPs easily accept changes to their equilibrium bond lengths, providing for large conformational freedom compared to other semiconductors with similar electronic properties.

The rich structural diversity, together with the material flexibility of HOIPs, may lead to *different phases being present locally* (i.e., multiple variants of the aristotype coexist) in HOIP films and surfaces. Indeed, theoretical work showed that XRD patterns are compatible with different coexisting phases³² and that on a sub-ps time scale systems can deviate from the ideal structure.³³ Moreover, the thermodynamic stability of HOIPs, quantified by the segregation energy of ABX₃ \rightarrow AX + BX₂, is very low.³⁴ Therefore, regions containing a fraction of the binary components (BX₂ and/or AX) and other complexes are another possibility discussed in the literature.³⁵ Practically, the local presence of secondary phases is especially relevant to HOIPs in which phase transitions can occur around room temperature, notably MAPbI₃ (Figure 1a).

3. MOLECULAR ROTATIONS AND OCTAHEDRAL DISTORTIONS

A peculiar aspect of HOIPs, compared to traditional semiconductors, is that the organic molecule may undergo significant rearrangements in the ideal crystal. This phenomenon was invoked for MAPbX₃ by Weber already in 1978:¹⁷ the nonspherical MA apparently does not distort the lead halide octahedra and significant MA motion explains the MA appearing to be spherical on average.¹⁷

To understand molecular rearrangements microscopically, recall that the potential energy surface of the molecule is influenced by interactions with neighboring BX₆ octahedra and molecule–molecule coupling. Dipole–dipole interactions of

molecules with distorted metal-halide octahedra could also play a role for lower-symmetry HOIP structures, with molecule–molecule coupling expected to be largely due to (screened) dipole–dipole interactions. Typical organic cations, notably MA, allow for several low-energy orientations as part of the perovskite structure, for example, aligned with corners, edges, or faces of the inorganic cages (Figure 2a).^{36,37} Theoretically,

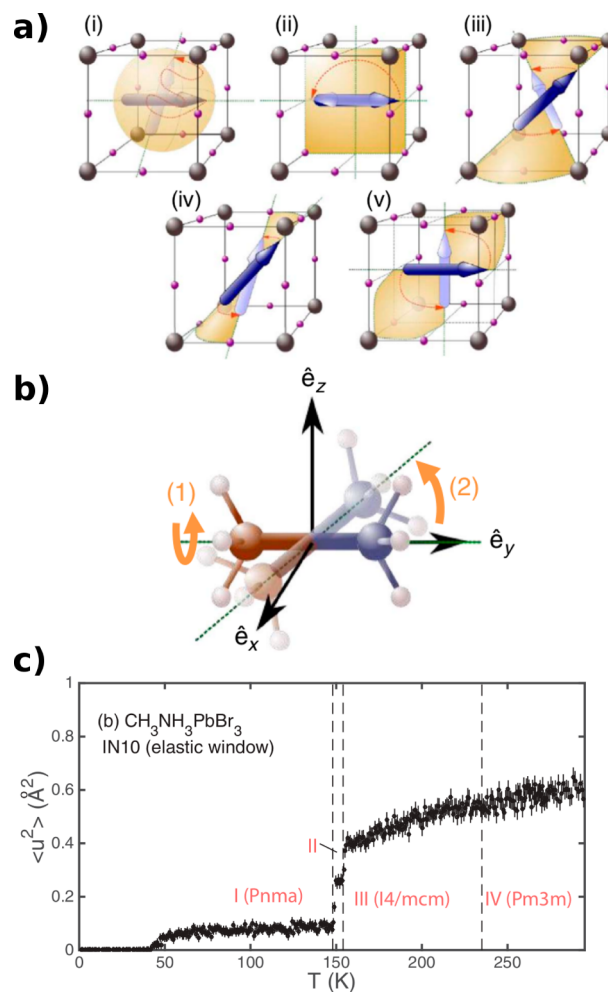


Figure 2. (a) Possible minimum-energy orientations and associated reorientation pathways, indexed from (i) to (v), for MA⁺ in MAPbI₃, based on rotation (2) in panel (b). (b) Two modes of rotation of MA⁺: (1) rotation of CH₃ or NH₃; (2) rotation of MA⁺, swapping locations of C and N. Reproduced with permission from ref 37. Copyright 2015 Macmillan Publishers Ltd.: Nature Communications. (c) Temperature-dependent mean-squared displacement of hydrogen atoms in MAPbBr₃ from neutron scattering. Reproduced with permission from ref 47. Copyright 2015 American Physical Society.

energy barriers for molecular rotation can be as low as several meV,^{10,19,20} suggesting significant movement of molecules at finite temperatures. Indeed, dielectric response and Raman spectroscopy results were interpreted by light exposure inducing or enhancing molecular rearrangements.^{38,39} Specific experimental evidence for molecular rearrangements is strong. Early measurements of ²H and ¹⁴N solid-state nuclear magnetic resonance spectra indicated rapid (sub-ps correlation times) molecular reorientations for the high-temperature phases of deuterated MAPbX₃, essentially independent of anion identity,⁴⁰ as confirmed recently.⁴¹ Temperature-dependent dielec-

tric response measurements of MAPbX_3 , analyzed using the Debye model, suggested dynamic disorder of MA dipoles involving ps relaxation.¹⁸ Dynamic disorder was also found in Cs-based all-inorganic crystals, suggesting that in lead-halide perovskites dynamic disorder is relevant irrespectively of the A-site cation.⁴²

Combining quasi-elastic neutron scattering measurements with Monte Carlo simulations for MAPbI_3 , Leguy et al. suggested two primary molecular motions dominant at room temperature (Figure 2b):³⁷ Motion of CH_3 and NH_3 about the C–N axis, or of the entire MA unit by rotation perpendicular to the C–N axis, which can occur via several possible pathways (Figure 2a). These two processes have different activation energies and thus occur at somewhat different time scales: the CH_3 - or NH_3 -related events occur at a possibly sub-ps time scale, whereas the realignment of the entire molecular unit is slower (3–14 ps), of similar magnitude to that deduced from molecular dynamics (MD)^{43,44} and recent experiments.^{45,46} One can therefore conclude that at room and higher temperatures, molecules in HOIPs have large conformational freedom. This agrees with Weber's analysis:¹⁷ *through extensive rotational dynamics of the molecular unit, the overall symmetry of HOIP crystals is increased.* More restricted molecular rotations correspond to a lower overall symmetry of the molecular unit and can be interpreted as symmetry-breaking distortions from the ideal thermally symmetrized A-site.

Consistent with this interpretation, molecular rotation in HOIPs was found to be strongly temperature-dependent, as deduced from the mean-squared displacement of the hydrogen atoms extracted from temperature-dependent neutron scattering (Figure 2c).⁴⁷ Once HOIPs are cooled and undergo phase transitions into tetragonal and orthorhombic structures, hydrogen displacements become smaller, indicating that rotations are restricted: experimental and theoretical results have shown that at lower temperatures molecular orientations are confined to high-symmetry directions of the crystal^{40,44} and reorientation energy barriers are enhanced.²¹

As T is lowered, the AX_{12} cuboctahedra shrink (due to BX_6 octahedral rotations), so there is less space for molecular rearrangements. It is therefore reasonable that *molecular and octahedral rearrangements are acting in concert*: molecules reorient over short times and, because BX_6 distortions and molecular rotations are coupled, bond lengths and angles of the BX_6 octahedra also change significantly.^{20,32,37} In this context, consider the related HOIP MAPbBr_3 , for which molecular rotations have been described as coupled to BX_6 octahedral distortions, resulting in coupling of order–disorder and displacive phase-transitions.⁴⁷ Interestingly, for MAPbI_3 , phonon spectra also indicate significant coupling between molecular and PbI_6 -related modes.¹⁶

Such cooperative action of molecular rotations and octahedral distortions suggests that HOIPs are dynamic materials: *a snapshot of a single structure cannot account for important dynamical effects* and, thus, does not provide sufficient insight into their properties. For example, first-principles calculations showed that the band gap magnitude, and even whether it is direct or slightly indirect, can change with molecular rotation.²⁰ This is interesting, given that the molecular electronic states do not contribute to the frontier levels in HOIPs (vide supra). However, consider that for a related Sn-based HOIP, molecular rearrangements influence the band structure⁴⁸ through electrostatic and hydrogen-bonding effects on the inorganic ions, which are primarily

responsible for the band-edge electronic structure.^{9,10,23,90} Therefore, structural fluctuations at room temperature can induce dynamical changes in important electronic-structure parameters, for example, band gap, effective masses, and possibly carrier lifetimes. Such effects have been reported also for Pb-based HOIPs based on MD, which at 320 K predict time-dependent band gap changes of 0.1–0.2 eV.^{32,33}

We speculate that the interplay of electronic and structural dynamical phenomena can result in a number of interesting electron–lattice coupling effects in HOIPs.⁴⁹ For example, scattering of charge-carriers by acoustic phonons may help understand some as-yet unexplained results for modest carrier mobilities of HOIPs.^{49,50} Polaronic effects in HOIPs could also be important and were invoked to explain low mobilities,^{49,51,52} light-induced changes of the low-frequency dielectric response,³⁹ and photostability due to coupling of light-generated carriers to polar fluctuations in the lattice.⁵³

Molecular rotations, octahedral distortions, and phase transitions are closely related to ferroelectricity, which for HOIPs is possible in principle because lower-temperature phases can crystallize in polar space groups.² Ferroelectricity in HOIPs has been studied based on Berry phase calculations, predicting polarization of ≈ 4 – $12 \mu\text{C}/\text{cm}^2$ for the lower-temperature phases of MAPbX_3 ($X = \text{I}, \text{Br}, \text{Cl}$),^{22,54,55} significantly lower than values reported for ferroelectric oxides, for example, BaTiO_3 . Measuring ferroelectric hysteresis in HOIPs is challenging, given their small band gap and relatively large number of mobile carriers, which can result in leakage currents.^{13,22} The ferroelectric nature of HOIPs is therefore currently disputed, with reports claiming either presence⁵⁶ or absence^{22,57} of ferroelectricity. Interestingly, Zhou et al.²¹ predict that in MAPbI_3 different molecular orientations have a larger impact on the polarization than lead displacements.

Given the molecular flexibility and rich structural diversity of HOIPs, large ferroelectric domains in HOIPs could indeed be difficult to stabilize over a sufficiently long time at room temperature. But one could also consider short-lived ferroelectric domains in HOIPs.^{24,36} Interestingly, long-range electrostatic interactions of molecular dipoles can induce polar domains via regions of (partially) aligned dipoles.^{36,58} Such domains can alter the HOIP band gap,⁵⁴ separate electron and hole wave functions (Figure 3a),⁵⁸ and suppress carrier recombination.^{59,60} Polar domains can also serve as channels for segregated transfer of electrons and holes, for example, by domain-wall formation (Figure 3b),^{24,36,54} which could partly explain the long carrier lifetimes of HOIPs. Ferroelectric phenomena in principle could also help explain the hysteresis observed in HOIP solar cells,⁶¹ although recent results put this into question.³⁷ Furthermore, ferroelectricity can give rise to a bulk PV effect, also discussed for HOIPs.^{62,63} The possibly strong impact of ferroelectricity and polar domains on charge-transport calls for establishing more definitive experimental evidence for its absence or presence in HOIPs, at best combined with advanced theory that can account for the structural fluctuations.

4. THE ROLE OF ION MIGRATION

For HOIPs, as for any semiconductor, knowledge of defects is crucial for understanding the electrical properties. Several defect-related observations have been reported, including very long charge-carrier diffusion lengths and low trap densities.^{64–66} Here, we focus on *migration of ionic defects*, invoked to explain phenomenological observations including hystere-

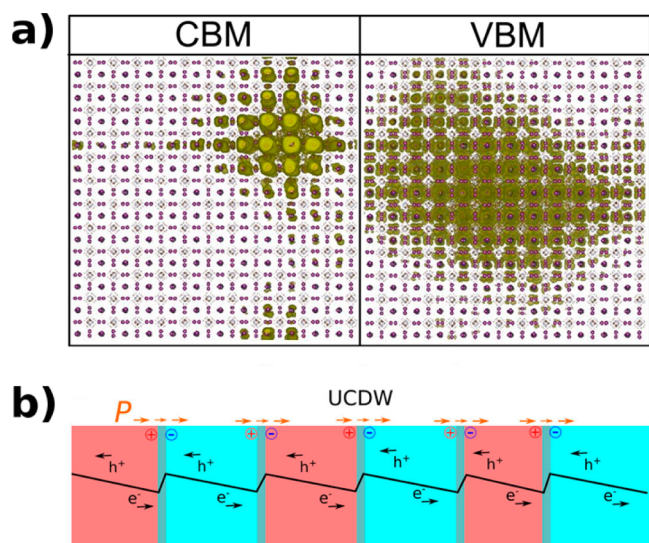


Figure 3. (a) Isosurface representation of the charge densities associated with the conduction band minimum (CBM) and valence band maximum (VBM) in a 20736-atom supercell of MAPbI₃ with MA randomly oriented along the eight $\langle 111 \rangle$ directions.⁵⁸ Reproduced with permission from ref 58. Copyright 2015 American Chemical Society. (b) Schematic illustration of steps in the electrostatic potential, causing electron–hole separations in an array of uncharged domain walls (UCDWs).⁵⁴ Reproduced with permission from ref 54. Copyright 2015 American Chemical Society.

sis^{61,67,68} (via ion-blocking contacts), switchable PV effects,^{69,70} and light-induced changes in structural^{38,69–72} and dielectric properties.³⁹ Whether (intrinsic or extrinsic) ions can diffuse at room temperature is, naturally, also relevant for material stability.

For some inorganic lead-halide perovskites⁷³ and lead dihalides,⁷⁴ ion migration has been investigated decades ago. These conduct anions through vacancies, with activation energies of ≈ 0.2 – 0.4 eV. For HOIPs, ionic conduction was proposed by Dualeh et al. based on impedance spectroscopy.⁷⁵ Recently, several experimental and theoretical studies presented more detailed evidence for *migration of intrinsic ionic defects* in HOIPs. Yang et al. measured temperature-dependent conductivities of MAPbI₃, showing an activation energy of ≈ 0.4 eV.⁷⁶ Using impedance spectroscopy and galvanostatic DC-measurements, they argued that MAPbI₃ is a mixed ionic-electronic conductor, with surprisingly large ionic conductivities in the dark, even surpassing the electronic ones.⁷⁶ Yuan et al. reported that the MAPbI₃ conductivity in the dark consists of two regions (Figure 4a):⁷⁷ the first (100–270 K) exhibits activation energies of ≈ 40 meV, assigned to electronic carriers, and the second (290–350 K) 10-fold larger ones (≈ 0.4 eV), assigned to ionic migration.⁷⁷

While these two studies present independent experimental evidence for ion migration with similar activation energies, they disagree on the diffusion constant (by some 3 orders of magnitude) and over *which ion moves*. Yang et al. used a solid-state Pb|MAPbI₃|AgI|Ag electrochemical cell and observed PbI₂ formation at the Pb|MAPbI₃ interface under bias, indicating that I[−] is the fastest intrinsic defect (Figure 4b).^{76,78} In contrast, using photothermal induced resonance microscopy, Yuan et al. concluded that MA⁺ migrates (see Figure 4c)⁷⁸ when the device is electrically poled.⁷⁷ They recently reported evidence

for iodide vacancy migration at elevated temperatures, relevant in the decomposition of MAPbI₃ under small electric fields.⁷⁹

Further results supporting either migration model have been found. It was argued that under illumination of mixed iodide-bromide films, halides can segregate into regions that are structurally different from the rest of the film (cf. section 2), influencing its optical properties.⁷² However, it was recently found that the organic cations (MA and formamidinium) can be rapidly exchanged, implying that organic cations may also be mobile.⁸⁰ Because HOIPs can easily deviate from their ideal bulk structure, as emphasized throughout, dynamical disorder, grain boundaries, and other nonidealities can also affect ion migration.

Recently, ion diffusion has been examined theoretically, allowing the identification of minimum energy paths and barriers for ideal structures. Calculations of defects and their diffusion are highly sensitive to the underlying theoretical and numerical framework. For HOIPs, migration barriers of 0.1–0.6 eV are found for iodide vacancies and of 0.5–0.9 eV for MA⁺ migration,^{78,81,82} which are quite large deviations. Thus, theoretically there is still significant uncertainty over which ions actually migrate.

We recently suggested an additional mechanism for ion migration: diffusion of hydrogen impurities, for example, protons (Figure 4d).⁸³ Hydrogen is an important *extrinsic defect* in inorganic semiconductors and some oxide perovskites are well-known proton conductors.⁸⁴ In HOIPs, hydrogen could therefore exist as extrinsic (introduced, e.g., via H₂O-induced partial decomposition of the HOIP, as speculated in ref 24) or as intrinsic defects (through the organic unit). Our calculations predicted low migration barriers (~ 0.1 – 0.2 eV) for H⁺ in MAPbI₃ and showed that diffusion mechanisms resemble those discussed for oxide proton conductors, involving transient H-bonds (Figure 4d).⁸³ We showed that differently charged defects prefer different sites (to be near ions of opposite charge), allowing for ionization-enhanced defect migration. This may be relevant for other defects and charging scenarios and has been supported by recent experiments.⁸⁵ Given that hydrogen impurities are difficult to control, H migration can complicate the interpretation of conductivity measurements, especially in light of recent findings on H₂O adsorption and associated degradation mechanisms.^{85–89}

5. SUMMARY AND CONCLUSIONS

In this Account, we provided an overview of structural dynamics of hybrid organic–inorganic perovskites (HOIPs), a family of materials that is highly interesting for applications in (opto)electronics and also puzzling from a scientific perspective. This is especially so considering a number of experimental observations that are atypical in the context of other highly efficient materials for PV.

We discussed crystal cohesion and bonding, showing that it is relatively weak, based on the mechanical properties of HOIPs and on first-principles calculations. This is especially relevant given that perovskites can access many lower-symmetry structures from an aristotype, which for HOIPs implies a large pool of structural motifs accessible at room temperature. In thin films, secondary structural phases could therefore exist. We discussed several findings on rotational dynamics of molecular cations in HOIPs, highlighting their strong connection with octahedral distortions, which can influence the electronic properties of HOIPs. Together with the notion of locally fluctuating regions bearing secondary phases, one may

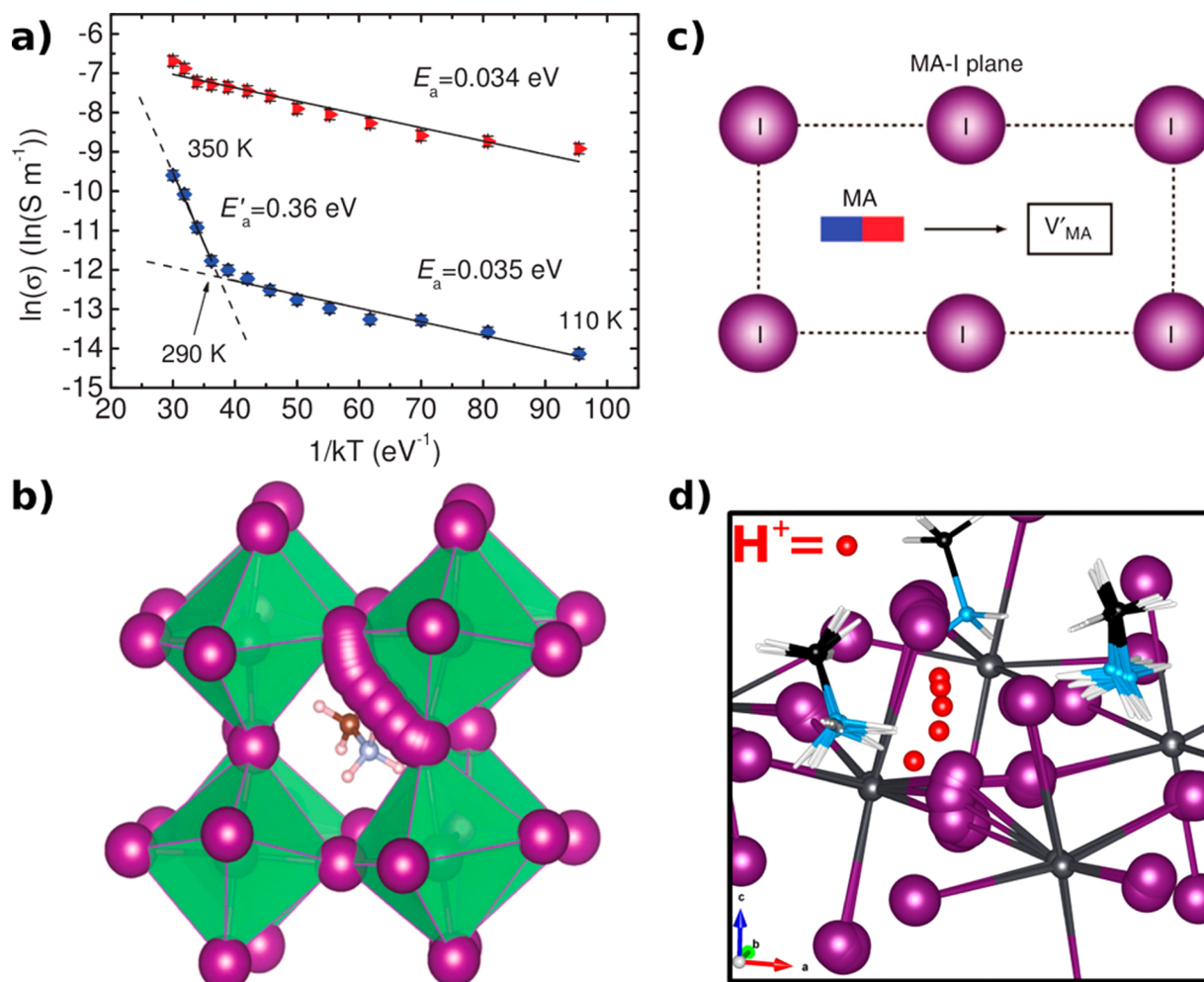


Figure 4. (a) Arrhenius plot of the electrical conductivity of MAPbI₃ in the dark (blue) and under illumination (red).⁷⁷ Reproduced with permission from ref 77. Copyright 2015 Wiley-VCH Verlag GmbH & Co. (b–d) Schematics of ionic diffusion mechanisms in MAPbI₃: migration of I vacancies (b),⁷⁸ MA vacancies (c),⁷⁸ and hydrogen interstitials (d).⁸³ Panels (b) and (d) show pathways with several geometries. Reproduced with permission from ref 78. Copyright 2015 Macmillan Publishers Ltd.: Nature Communications. Adapted from ref 83. Copyright 2015 Wiley-VCH Verlag GmbH & Co.

envison domains that can locally facilitate (or hinder) charge-carrier transport and/or separation.

Finally, more and more evidence points toward significant migration of ionic species in HOIPs. It is unclear which species is/are moving, but experimental and theoretical studies proposed several different defect models, including halide and molecular vacancies, as well as hydrogen impurities.

From this perspective, HOIPs emerge as materials that are highly flexible mechanically and structurally dynamic. Given the potentially strong impact of structural fluctuations on charge-transport and optical properties, it appears necessary to call for a change in the perception of HOIPs: Envisioning them in one specific structure at a given temperature, distorted only by small and harmonic changes, clearly falls short of recognizing dynamical phenomena as an outstanding characteristic of these materials.

We conclude that HOIPs are “on the move” and hope that our emphasis on this issue will trigger further experimental and theoretical work to establish a microscopic understanding of their structural dynamics. We believe that this will be relevant to open questions in the field, some of which we have outlined throughout this Account. It may furthermore shine light on an

important and curious property: that a high-quality semiconductor can be processed from solution by simple means.

AUTHOR INFORMATION

Corresponding Authors

*E-mail: david.egger@weizmann.ac.il.

*E-mail: rappe@sas.upenn.edu.

*E-mail: leeor.kronik@weizmann.ac.il.

Notes

The authors declare no competing financial interest.

Biographies

David A. Egger received his Ph.D. in Physics in 2013 from Graz University of Technology, Austria. Currently, he is a Postdoctoral Fellow at the Department of Materials and Interfaces at the Weizmann Institute of Science, supported by a Schrödinger Fellowship of the Austrian Science Fund. In 2014, he received the Koshland Prize of the Weizmann Institute of Science.

Andrew M. Rappe received his Ph.D. in Physics and Chemistry in 1992 from MIT. He is Professor of Chemistry and Professor of Materials Science and Engineering at the University of Pennsylvania,

as well as founding co-director of the VIPER Program. He is a Fellow of the American Physical Society, a Sloan Fellow, and a Dreyfus Teacher-Scholar. He was awarded a Weston Visiting Professorship at the Weizmann Institute of Science in 2014.

Leor Kronik obtained his Ph.D. in Physical Electronics in 1996 at Tel Aviv University. Presently, he leads a group devoted to the quantum theory of real materials at the Department of Materials and Interfaces, Weizmann Institute of Science. He is a Fellow of the American Physical Society and a Member of the Israeli Young National Academy and has received the Young Scientist Award of the Israel Chemical Society (2010) and the Young Scientist Krill Prize of the Wolf Foundation (2006).

ACKNOWLEDGMENTS

D.A.E. and L.K. were supported by a research grant from Dana and Yossie Hollander and by the Austrian Science Fund (FWF):J3608-N20. A.M.R. was supported by the US Office of Naval Research, Grant N00014-14-1-0761.

REFERENCES

- (1) Mitzi, D. B. Synthesis, Structure, and Properties of Organic-Inorganic Perovskites and Related Materials. In *Progress in Inorganic Chemistry*; Karlin, K. D., Ed.; John Wiley & Sons, Inc.: Hoboken, NJ, 1999; Vol. 48, pp 1–121.
- (2) Stoumpos, C. C.; Malliakas, C. D.; Kanatzidis, M. G. Semiconducting Tin and Lead Iodide Perovskites with Organic Cations: Phase Transitions, High Mobilities, and Near-Infrared Photoluminescent Properties. *Inorg. Chem.* **2013**, *52*, 9019–9038.
- (3) Brenner, T. M.; Egger, D. A.; Kronik, L.; Hodes, G.; Cahen, D. Hybrid Organic-inorganic Perovskites: Low-Cost Semiconductors with Intriguing Charge-Transport Properties. *Nat. Rev. Mater.* **2016**, *1*, 15007.
- (4) Park, N.-G. Organometal Perovskite Light Absorbers Toward a 20% Efficiency Low-Cost Solid-State Mesoscopic Solar Cell. *J. Phys. Chem. Lett.* **2013**, *4*, 2423–2429.
- (5) Gao, P.; Grätzel, M.; Nazeeruddin, M. K. Organohalide Lead Perovskites for Photovoltaic Applications. *Energy Environ. Sci.* **2014**, *7*, 2448–2463.
- (6) Stranks, S. D.; Snaith, H. J. Metal-Halide Perovskites for Photovoltaic and Light-Emitting Devices. *Nat. Nanotechnol.* **2015**, *10*, 391–402.
- (7) Miyasaka, T. Perovskite Photovoltaics: Rare Functions of Organo Lead Halide in Solar Cells and Optoelectronic Devices. *Chem. Lett.* **2015**, *44*, 720–729.
- (8) See http://www.nrel.gov/ncpv/images/efficiency_chart.jpg. (accessed Jan 27, 2016).
- (9) Umebayashi, T.; Asai, K.; Kondo, T.; Nakao, A. Electronic Structures of Lead Iodide Based Low-Dimensional Crystals. *Phys. Rev. B: Condens. Matter Mater. Phys.* **2003**, *67*, 155405.
- (10) Chang, Y. H.; Park, C. H.; Matsuishi, K. First-Principles Study of the Structural and the Electronic Properties of the Lead-Halide-Based Inorganic-Organic Perovskites (CH₃NH₃)PbX₃ and CsPbX₃ (X = Cl, Br, I). *J.-Korean Phys. Soc.* **2004**, *44*, 889–893.
- (11) Goldschmidt, V. M. Die Gesetze der Krystallochemie. *Naturwissenschaften* **1926**, *14*, 477–485.
- (12) Brehm, J. A.; Bennett, J. W.; Schoenberg, M. R.; Grinberg, I.; Rappe, A. M. The Structural Diversity of ABS₃ Compounds with d₀ Electronic Configuration for the B-Cation. *J. Chem. Phys.* **2014**, *140*, 224703.
- (13) *Physics of Ferroelectrics; Topics in Applied Physics*; Rabe, K. M., Ahn, C. H., Triscone, J.-M., Eds.; Springer: Berlin, 2007; Vol. 105.
- (14) Glazer, A. M. The Classification of Tilted Octahedra in Perovskites. *Acta Crystallogr., Sect. B: Struct. Crystallogr. Cryst. Chem.* **1972**, *28*, 3384–3392.
- (15) Stokes, H. T.; Kisi, E. H.; Hatch, D. M.; Howard, C. J. Group-Theoretical Analysis of Octahedral Tilting in Ferroelectric Perovskites. *Acta Crystallogr., Sect. B: Struct. Sci.* **2002**, *58*, 934–938.
- (16) Brivio, F.; Frost, J. M.; Skelton, J. M.; Jackson, A. J.; Weber, O. J.; Weller, M. T.; Goñi, A. R.; Leguy, A. M. A.; Barnes, P. R. F.; Walsh, A. Lattice Dynamics and Vibrational Spectra of the Orthorhombic, Tetragonal, and Cubic Phases of Methylammonium Lead Iodide. *Phys. Rev. B: Condens. Matter Mater. Phys.* **2015**, *92*, 144308.
- (17) Weber, D. CH₃NH₃PbX₃, a Pb(II)-System with Cubic Perovskite Structure. *Z. Naturforsch., B: J. Chem. Sci.* **1978**, *33*, 1443–1445.
- (18) Poglitsch, A.; Weber, D. Dynamic Disorder in Methylammoniumtrihalogenoplumbates (II) Observed by Millimeter-Wave Spectroscopy. *J. Chem. Phys.* **1987**, *87*, 6373.
- (19) Brivio, F.; Walker, A. B.; Walsh, A. Structural and Electronic Properties of Hybrid Perovskites for High-Efficiency Thin-Film Photovoltaics from First-Principles. *APL Mater.* **2013**, *1*, 042111.
- (20) Motta, C.; El-Mellouhi, F.; Kais, S.; Tabet, N.; Alharbi, F.; Sanvito, S. Revealing the Role of Organic Cations in Hybrid Halide Perovskite CH₃NH₃PbI₃. *Nat. Commun.* **2015**, *6*, 7026.
- (21) Zhou, Y.; Huang, F.; Cheng, Y.-B.; Gray-Weale, A. Photovoltaic Performance and the Energy Landscape of CH₃NH₃PbI₃. *Phys. Chem. Chem. Phys.* **2015**, *17*, 22604–22615.
- (22) Fan, Z.; Xiao, J.; Sun, K.; Chen, L.; Hu, Y.; Ouyang, J.; Ong, K. P.; Zeng, K.; Wang, J. Ferroelectricity of CH₃NH₃PbI₃ Perovskite. *J. Phys. Chem. Lett.* **2015**, *6*, 1155–1161.
- (23) Brivio, F.; Butler, K. T.; Walsh, A.; van Schilfgaarde, M. Relativistic Quasiparticle Self-Consistent Electronic Structure of Hybrid Halide Perovskite Photovoltaic Absorbers. *Phys. Rev. B: Condens. Matter Mater. Phys.* **2014**, *89*, 155204.
- (24) Frost, J. M.; Butler, K. T.; Brivio, F.; Hendon, C. H.; van Schilfgaarde, M.; Walsh, A. Atomistic Origins of High-Performance in Hybrid Halide Perovskite Solar Cells. *Nano Lett.* **2014**, *14*, 2584–2590.
- (25) Wang, Y.; Gould, T.; Dobson, J. F.; Zhang, H.; Yang, H.; Yao, X.; Zhao, H. Density Functional Theory Analysis of Structural and Electronic Properties of Orthorhombic Perovskite CH₃NH₃PbI₃. *Phys. Chem. Chem. Phys.* **2014**, *16*, 1424.
- (26) Egger, D. A.; Kronik, L. Role of Dispersive Interactions in Determining Structural Properties of Organic-Inorganic Halide Perovskites: Insights from First-Principles Calculations. *J. Phys. Chem. Lett.* **2014**, *5*, 2728–2733.
- (27) Menéndez-Proupin, E.; Palacios, P.; Wahnón, P.; Conesa, J. C. Self-Consistent Relativistic Band Structure of the CH₃NH₃PbI₃ Perovskite. *Phys. Rev. B: Condens. Matter Mater. Phys.* **2014**, *90*, 045207.
- (28) Lee, Y.; Mitzi, D. B.; Barnes, P. W.; Vogt, T. Pressure-Induced Phase Transitions and Templating Effect in Three-Dimensional Organic-Inorganic Hybrid Perovskites. *Phys. Rev. B: Condens. Matter Mater. Phys.* **2003**, *68*, 020103.
- (29) Feng, J. Mechanical Properties of Hybrid Organic-Inorganic CH₃NH₃BX₃ (B = Sn, Pb; X = Br, I) Perovskites for Solar Cell Absorbers. *APL Mater.* **2014**, *2*, 081801.
- (30) Sun, S.; Fang, Y.; Kieslich, G.; White, T. J.; Cheetham, A. K. Mechanical Properties of Organic-inorganic Halide Perovskites, CH₃NH₃PbX₃ (X = I, Br and Cl), by Nanoindentation. *J. Mater. Chem. A* **2015**, *3*, 18450–18455.
- (31) Rakita, Y.; Cohen, S. R.; Kedem, N. K.; Hodes, G.; Cahen, D. Mechanical Properties of APbX₃ (A = Cs or CH₃NH₃; X = I or Br) Perovskite Single Crystals. *MRS Commun.* **2015**, *5*, 623–629.
- (32) Quarti, C.; Mosconi, E.; De Angelis, F. Interplay of Orientational Order and Electronic Structure in Methylammonium Lead Iodide: Implications for Solar Cell Operation. *Chem. Mater.* **2014**, *26*, 6557–6569.
- (33) Quarti, C.; Mosconi, E.; Ball, J. M.; D’Innocenzo, V.; Tao, C.; Pathak, S.; Snaith, H. J.; Petrozza, A.; De Angelis, F. Structural and Optical Properties of Methylammonium Lead Iodide across the Tetragonal to Cubic Phase Transition: Implications for Perovskite Solar Cells. *Energy Environ. Sci.* **2016**, *9*, 155–163.

- (34) Zhang, Y.-Y.; Chen, S.; Xu, P.; Xiang, H.; Gong, X.-G.; Walsh, A.; Wei, S.-H. Intrinsic Instability of the Hybrid Halide Perovskite Semiconductor $\text{CH}_3\text{NH}_3\text{PbI}_3$. **2015**, arXiv:1506.01301. arXiv.org e-Print archive. <http://arxiv.org/abs/1506.01301>.
- (35) Stamplecoskie, K. G.; Manser, J. S.; Kamat, P. V. Dual Nature of the Excited State in Organic–inorganic Lead Halide Perovskites. *Energy Environ. Sci.* **2015**, *8*, 208–215.
- (36) Frost, J. M.; Butler, K. T.; Walsh, A. Molecular Ferroelectric Contributions to Anomalous Hysteresis in Hybrid Perovskite Solar Cells. *APL Mater.* **2014**, *2*, 081506.
- (37) Leguy, A. M. A.; Frost, J. M.; McMahon, A. P.; Sakai, V. G.; Kochemann, W.; Law, C.; Li, X.; Foglia, F.; Walsh, A.; O'Regan, B. C.; Nelson, J.; Cabral, J. T.; Barnes, P. R. F. The Dynamics of Methylammonium Ions in Hybrid Organic–inorganic Perovskite Solar Cells. *Nat. Commun.* **2015**, *6*, 7124.
- (38) Gottesman, R.; Haltzi, E.; Gouda, L.; Tirosh, S.; Bouhadana, Y.; Zaban, A.; Mosconi, E.; De Angelis, F. Extremely Slow Photoconductivity Response of $\text{CH}_3\text{NH}_3\text{PbI}_3$ Perovskites Suggesting Structural Changes under Working Conditions. *J. Phys. Chem. Lett.* **2014**, *5*, 2662–2669.
- (39) Juarez-Perez, E. J.; Sanchez, R. S.; Badia, L.; Garcia-Belmonte, G.; Kang, Y. S.; Mora-Sero, I.; Bisquert, J. Photoinduced Giant Dielectric Constant in Lead Halide Perovskite Solar Cells. *J. Phys. Chem. Lett.* **2014**, *5*, 2390–2394.
- (40) Wasylishen, R. E.; Knop, O.; Macdonald, J. B. Cation Rotation in Methylammonium Lead Halides. *Solid State Commun.* **1985**, *56*, 581–582.
- (41) Baikie, T.; Barrow, N. S.; Fang, Y.; Keenan, P. J.; Slater, P. R.; Piltz, R. O.; Gutmann, M.; Mhaisalkar, S. G.; White, T. J. A Combined Single Crystal neutron/x-Ray Diffraction and Solid-State Nuclear Magnetic Resonance Study of the Hybrid Perovskites $\text{CH}_3\text{NH}_3\text{PbX}_3$ ($X = \text{I, Br and Cl}$). *J. Mater. Chem. A* **2015**, *3*, 9298–9307.
- (42) Guo, Y.; Yaffe, O.; Norman, Z.; Hull, T.; Semonin, O. E.; Stoumpos, K.; Kanatzidis, M. G.; Owen, J.; Heinz, T. F.; Pimenta, M. A.; Brus, L. E.; Low Frequency Raman Study of Dynamic Disorder in Lead-Halide Perovskite Single Crystals. Paper NN14.05, MRS Fall 2015 Meeting, Boston, MA Dec. 2015, <http://www.mrs.org/fall-2015-Program-NN/>.
- (43) Mosconi, E.; Quarti, C.; Ivanovska, T.; Ruani, G.; De Angelis, F. Structural and Electronic Properties of Organo-Halide Lead Perovskites: A Combined IR-Spectroscopy and Ab Initio Molecular Dynamics Investigation. *Phys. Chem. Chem. Phys.* **2014**, *16*, 16137.
- (44) Mattoni, A.; Filippetti, A.; Saba, M. I.; Delugas, P. Methylammonium Rotational Dynamics in Lead Halide Perovskite by Classical Molecular Dynamics: The Role of Temperature. *J. Phys. Chem. C* **2015**, *119*, 17421–17428.
- (45) Bakulin, A. A.; Selig, O.; Bakker, H. J.; Rezus, Y. L. A.; Müller, C.; Glaser, T.; Lovrincic, R.; Sun, Z.; Chen, Z.; Walsh, A.; Frost, J. M.; Jansen, T. L. C. Real-Time Observation of Organic Cation Reorientation in Methylammonium Lead Iodide Perovskites. *J. Phys. Chem. Lett.* **2015**, *6*, 3663–3669.
- (46) Chen, T.; Foley, B. J.; Ipek, B.; Tyagi, M.; Copley, J. R. D.; Brown, C. M.; Choi, J. J.; Lee, S.-H. Rotational Dynamics of Organic Cations in $\text{CH}_3\text{NH}_3\text{PbI}_3$ Perovskite. *Phys. Chem. Chem. Phys.* **2015**, *17*, 31278–31286.
- (47) Swanson, I. P.; Stock, C.; Parker, S. F.; Van Eijck, L.; Russina, M.; Taylor, J. W. From Soft Harmonic Phonons to Fast Relaxational Dynamics in $\text{CH}_3\text{NH}_3\text{PbBr}_3$. *Phys. Rev. B: Condens. Matter Mater. Phys.* **2015**, *92*, 100303.
- (48) Knutson, J. L.; Martin, J. D.; Mitzi, D. B. Tuning the Band Gap in Hybrid Tin Iodide Perovskite Semiconductors Using Structural Templating. *Inorg. Chem.* **2005**, *44*, 4699–4705.
- (49) Brenner, T. M.; Egger, D. A.; Rappe, A. M.; Kronik, L.; Hodes, G.; Cahen, D. Are Mobilities in Hybrid Organic–Inorganic Halide Perovskites Actually “High”? *J. Phys. Chem. Lett.* **2015**, *6*, 4754–4757.
- (50) Karakus, M.; Jensen, S. A.; D'Angelo, F.; Turchinovich, D.; Bonn, M.; Cánovas, E. Phonon–Electron Scattering Limits Free Charge Mobility in Methylammonium Lead Iodide Perovskites. *J. Phys. Chem. Lett.* **2015**, *6* (24), 4991–4996.
- (51) Chen, Y.; Yi, H. T.; Wu, X.; Haroldson, R.; Gartstein, Y.; Zakhidov, A.; Zhu, X.-Y.; Podzorov, V. Ultra-long carrier lifetimes and diffusion lengths in hybrid perovskites revealed by steady-state Hall effect and photoconductivity measurements. Submitted.
- (52) Zhu, X.-Y.; Podzorov, V. Charge Carriers in Hybrid Organic–Inorganic Lead Halide Perovskites Might Be Protected as Large Polarons. *J. Phys. Chem. Lett.* **2015**, *6*, 4758–4761.
- (53) Tretiak, S. Private communication, 2015.
- (54) Liu, S.; Zheng, F.; Koocher, N. Z.; Takenaka, H.; Wang, F.; Rappe, A. M. Ferroelectric Domain Wall Induced Band Gap Reduction and Charge Separation in Organometal Halide Perovskites. *J. Phys. Chem. Lett.* **2015**, *6*, 693–699.
- (55) Stroppa, A.; Quarti, C.; De Angelis, F.; Picozzi, S. Ferroelectric Polarization of $\text{CH}_3\text{NH}_3\text{PbI}_3$: A Detailed Study Based on Density Functional Theory and Symmetry Mode Analysis. *J. Phys. Chem. Lett.* **2015**, *6*, 2223–2231.
- (56) Kutes, Y.; Ye, L.; Zhou, Y.; Pang, S.; Huey, B. D.; Padture, N. P. Direct Observation of Ferroelectric Domains in Solution-Processed $\text{CH}_3\text{NH}_3\text{PbI}_3$ Perovskite Thin Films. *J. Phys. Chem. Lett.* **2014**, *5*, 3335–3339.
- (57) Ehre, D.; Rakita, Y.; Hodes, G.; Cahen, D.; Lubomirsky, I.; *Direct Experimental Evidence for Absence of Polarity in $\text{CH}_3\text{NH}_3\text{PbBr}_3$ Crystals*. Symposium NN, MRS Fall 2015 Meeting, Boston, MA Dec. 2015, see <http://www.mrs.org/fall-2015-Rump-Session/>.
- (58) Ma, J.; Wang, L.-W. Nanoscale Charge Localization Induced by Random Orientations of Organic Molecules in Hybrid Perovskite $\text{CH}_3\text{NH}_3\text{PbI}_3$. *Nano Lett.* **2015**, *15*, 248–253.
- (59) Kepenekian, M.; Robles, R.; Katan, C.; Saporì, D.; Pedesseau, L.; Even, J. Rashba and Dresselhaus Effects in Hybrid Organic-Inorganic Perovskites: From Basics to Devices. *ACS Nano* **2015**, *9*, 11557–11567.
- (60) Zheng, F.; Tan, L. Z.; Liu, S.; Rappe, A. M. Rashba Spin–Orbit Coupling Enhanced Carrier Lifetime in $\text{CH}_3\text{NH}_3\text{PbI}_3$. *Nano Lett.* **2015**, *15*, 7794–7800.
- (61) Snaith, H. J.; Abate, A.; Ball, J. M.; Eperon, G. E.; Leijtens, T.; Noel, N. K.; Stranks, S. D.; Wang, J. T.-W.; Wojciechowski, K.; Zhang, W. Anomalous Hysteresis in Perovskite Solar Cells. *J. Phys. Chem. Lett.* **2014**, *5*, 1511–1515.
- (62) Zheng, F.; Takenaka, H.; Wang, F.; Koocher, N. Z.; Rappe, A. M. First-Principles Calculation of the Bulk Photovoltaic Effect in $\text{CH}_3\text{NH}_3\text{PbI}_3$ and $\text{CH}_3\text{NH}_3\text{PbI}_{3-x}\text{Cl}_x$. *J. Phys. Chem. Lett.* **2015**, *6*, 31–37.
- (63) Butler, K. T.; Frost, J. M.; Walsh, A. Ferroelectric Materials for Solar Energy Conversion: Photoferroics Revisited. *Energy Environ. Sci.* **2015**, *8*, 838–848.
- (64) Stranks, S. D.; Eperon, G. E.; Grancini, G.; Menelaou, C.; Alcocer, M. J.; Leijtens, T.; Herz, L. M.; Petrozza, A.; Snaith, H. J. Electron-Hole Diffusion Lengths Exceeding 1 Micrometer in an Organometal Trihalide Perovskite Absorber. *Science* **2013**, *342*, 341–344.
- (65) Shi, D.; et al. Low Trap-State Density and Long Carrier Diffusion in Organolead Trihalide Perovskite Single Crystals. *Science* **2015**, *347*, 519–522.
- (66) Dong, Q.; Fang, Y.; Shao, Y.; Mulligan, P.; Qiu, J.; Cao, L.; Huang, J. Electron-Hole Diffusion Lengths > 175 μm in Solution-Grown $\text{CH}_3\text{NH}_3\text{PbI}_3$ Single Crystals. *Science* **2015**, *347*, 967–970.
- (67) Unger, E. L.; Hoke, E. T.; Bailie, C. D.; Nguyen, W. H.; Bowring, A. R.; Heumüller, T.; Christoforo, M. G.; McGehee, M. D. Hysteresis and Transient Behavior in Current–voltage Measurements of Hybrid-Perovskite Absorber Solar Cells. *Energy Environ. Sci.* **2014**, *7*, 3690–3698.
- (68) Tress, W.; Marinova, N.; Moehl, T.; Zakeeruddin, S. M.; Nazeeruddin, M. K.; Grätzel, M. Understanding the Rate-Dependent J–V Hysteresis, Slow Time Component, and Aging in $\text{CH}_3\text{NH}_3\text{PbI}_3$ Perovskite Solar Cells: The Role of a Compensated Electric Field. *Energy Environ. Sci.* **2015**, *8*, 995–1004.
- (69) Xiao, Z.; Yuan, Y.; Shao, Y.; Wang, Q.; Dong, Q.; Bi, C.; Sharma, P.; Gruverman, A.; Huang, J. Giant Switchable Photovoltaic

Effect in Organometal Trihalide Perovskite Devices. *Nat. Mater.* **2014**, *14*, 193–198.

(70) Deng, Y.; Xiao, Z.; Huang, J. Light-Induced Self-Poling Effect on Organometal Trihalide Perovskite Solar Cells for Increased Device Efficiency and Stability. *Adv. Energy Mater.* **2015**, *5*, 1500721.

(71) Gottesman, R.; Gouda, L.; Kalanoor, B. S.; Haltzi, E.; Tirosh, S.; Rosh-Hodesh, E.; Tischler, Y.; Zaban, A.; Quarti, C.; Mosconi, E.; De Angelis, F. Photoinduced Reversible Structural Transformations in Free-Standing $\text{CH}_3\text{NH}_3\text{PbI}_3$ Perovskite Films. *J. Phys. Chem. Lett.* **2015**, *6*, 2332–2338.

(72) Hoke, E. T.; Slotcavage, D. J.; Dohner, E. R.; Bowring, A. R.; Karunadasa, H. I.; McGehee, M. D. Reversible Photo-Induced Trap Formation in Mixed-Halide Hybrid Perovskites for Photovoltaics. *Chem. Sci.* **2015**, *6*, 613–617.

(73) Mizusaki, J.; Arai, K.; Fueki, K. Ionic Conduction of the Perovskite-Type Halides. *Solid State Ionics* **1983**, *11*, 203–211.

(74) Verwey, J. F.; Schoonman, J. Crystal Growth, Ionic Conductivity, and Photolysis of Pure and Impurity-Doped Lead Bromide Single Crystals. *Physica* **1967**, *35*, 386–394.

(75) Dualeh, A.; Moehl, T.; Tétreault, N.; Teuscher, J.; Gao, P.; Nazeeruddin, M. K.; Grätzel, M. Impedance Spectroscopic Analysis of Lead Iodide Perovskite-Sensitized Solid-State Solar Cells. *ACS Nano* **2014**, *8*, 362–373.

(76) Yang, T.-Y.; Gregori, G.; Pellet, N.; Grätzel, M.; Maier, J. The Significance of Ion Conduction in a Hybrid Organic-Inorganic Lead-Iodide-Based Perovskite Photosensitizer. *Angew. Chem.* **2015**, *127*, 8016–8021.

(77) Yuan, Y.; Chae, J.; Shao, Y.; Wang, Q.; Xiao, Z.; Centrone, A.; Huang, J. Photovoltaic Switching Mechanism in Lateral Structure Hybrid Perovskite Solar Cells. *Adv. Energy Mater.* **2015**, *5*, 1500615.

(78) Eames, C.; Frost, J. M.; Barnes, P. R. F.; O'Regan, B. C.; Walsh, A.; Islam, M. S. Ionic Transport in Hybrid Lead Iodide Perovskite Solar Cells. *Nat. Commun.* **2015**, *6*, 7497.

(79) Yuan, Y.; Wang, Q.; Shao, Y.; Lu, H.; Li, T.; Gruverman, A.; Huang, J. Electric-Field-Driven Reversible Conversion Between Methylammonium Lead Triiodide Perovskites and Lead Iodide at Elevated Temperatures. *Adv. Energy Mater.* **2016**, *6*, 1501803.

(80) Eperon, G. E.; Beck, C. E.; Snaith, H. J. Cation Exchange for Thin Film Lead Iodide Perovskite Interconversion. *Mater. Horiz.* **2016**, *3*, 63–71.

(81) Azpiroz, J. M.; Mosconi, E.; Bisquert, J.; De Angelis, F. Defect Migration in Methylammonium Lead Iodide and Its Role in Perovskite Solar Cell Operation. *Energy Environ. Sci.* **2015**, *8*, 2118–2127.

(82) Haruyama, J.; Sodeyama, K.; Han, L.; Tateyama, Y. First-Principles Study of Ion Diffusion in Perovskite Solar Cell Sensitizers. *J. Am. Chem. Soc.* **2015**, *137*, 10048–10051.

(83) Egger, D. A.; Kronik, L.; Rappe, A. M. Theory of Hydrogen Migration in Organic-Inorganic Halide Perovskites. *Angew. Chem., Int. Ed.* **2015**, *54*, 12437–12441.

(84) Kreuer, K. D. Proton Conducting Oxides. *Annu. Rev. Mater. Res.* **2003**, *33*, 333–359.

(85) Müller, C.; Glaser, T.; Plogmeyer, M.; Sendner, M.; Döring, S.; Bakulin, A. A.; Brzuska, C.; Scheer, R.; Pshenichnikov, M. S.; Kowalsky, W.; Pucci, A.; Lovrinčić, R. Water Infiltration in Methylammonium Lead Iodide Perovskite: Fast and Inconspicuous. *Chem. Mater.* **2015**, *27*, 7835–7841.

(86) Mosconi, E.; Azpiroz, J. M.; De Angelis, F. *Ab Initio* Molecular Dynamics Simulations of Methylammonium Lead Iodide Perovskite Degradation by Water. *Chem. Mater.* **2015**, *27*, 4885–4892.

(87) Koocher, N. Z.; Saldana-Greco, D.; Wang, F.; Liu, S.; Rappe, A. M. Polarization Dependence of Water Adsorption to $\text{CH}_3\text{NH}_3\text{PbI}_3$ (001) Surfaces. *J. Phys. Chem. Lett.* **2015**, *6*, 4371–4378.

(88) Deretzis, I.; Alberti, A.; Pellegrino, G.; Smecca, E.; Giannazzo, F.; Sakai, N.; Miyasaka, T.; La Magna, A. Atomistic Origins of $\text{CH}_3\text{NH}_3\text{PbI}_3$ Degradation to PbI_2 in Vacuum. *Appl. Phys. Lett.* **2015**, *106*, 131904.

(89) Tong, C.-J.; Geng, W.; Tang, Z.-K.; Yam, C.-Y.; Fan, X.-L.; Liu, J.; Lau, W.-M.; Liu, L.-M. Uncovering the Veil of the Degradation in

Perovskite $\text{CH}_3\text{NH}_3\text{PbI}_3$ upon Humidity Exposure: A First-Principles Study. *J. Phys. Chem. Lett.* **2015**, *6*, 3289–3295.

(90) Du, M. H. Efficient Carrier Transport in Halide Perovskites: Theoretical Perspectives. *J. Mater. Chem. A* **2014**, *2*, 9091–9098.